Pergamon

Building and Environment, Vol. 32, No. 2, pp. 137–148, 1997

Printed in Great Britain
0360–1323/97 $17.00+0.00

PII: S0360–1323(96)00039–X

Study of Coupled Energy Saving Systems Sensitivity Factor Analysis

L. SERRES*
A. TROMBE*
J. H. CONILH*

(*Received* 13 *July* 1995; *revised* 5 *November* 1995; *accepted* 21 *October* 1996)

This study was carried out on a real site of a gymnasium situated in the centre of France. The building is equipped with two remarkable energy saving devices running together: a ventilated roof and an air–earth heat exchanger. Experimental and theoretical studies were done on these two energy saving systems and a sensitivity factor analysis was performed. First, each component was modelled in order to (1) determine the component's contribution to the energy savings; and (2) indicate the relative importance of different types of heat transfer which occur in the ventilated roof. Then, several types of fresh air preheating were studied, varying the heating control temperature of the building. The main results show that the economy of fresh air preheating can vary with the system used, and indicate the reasons for the lack of efficiency of some systems. Finally, fresh air introduction into the gymnasium was optimized. The combined influences of ventilation intermittency and climate on the global theoretical consumptions for the building were studied. It was shown that the optimization of air introduction into the gymnasium has no influence on the energy consumption of the building for a rather cold climate. On the other hand, for a warmer climate, significant energy savings can be obtained.

In conclusion, this study points out the general interest of simulation for new building designs. However, it can be also used for existing buildings to give significant information about equipment weaknesses and, of course, about improvements to be made.

NOMENCLATURE

C_p	specific heat of air (J/kg · K)
H_{la}	heat exchange coefficient of air gap (W/m^2 · K)
H_{ci}	convective heat exchange coefficient of inside surfaces of building (W/m^2 · K)
H_i	convective heat exchange coefficient inside tube of buried pipe system (W/m^2 · K)
H_{ce}	outside heat convective exchange coefficient of ventilated air gap (W/m^2 · K)
H_{cse}	inside convective heat exchange coefficient of air gap near top covering(W/m^2 · K)
H_{clv}	inside convective heat exchange coefficient of air gap near glass wool (W/m^2 · K)
H_{re}	outside radiative heat exchange coefficient (W/m^2 · K)
H_{ri}	inside radiative heat exchange coefficient (W/m^2 · K)
H_{rlv}	linearized infrared radiative coefficient of air gap from glass wool to metal covering (W/m^4 · K)
H_{rse}	linearized infrared radiative coefficient of air gap from metal covering to glass wool (W/m^4 · K)
L	breadth of roof (m)
$L(i)$	length of an element of roof (m)
Nu	Nusselt number
P	internal circumference of pipes (m)
Pr	Prandtl number
m	flow rate in air gap (kg/s)
R_i	thermal resistance of glass wool (m^2 · K/W)
R_e	thermal resistance of iron covering (m^2 · K/W)
Rey	Reynolds number
T_{ela}	inlet temperature of air gap (°C)
T_{epuits}	inlet temperature of buried pipe system (°C)
T_{int}, T_{ext}	respective values of inside and outside ambient temperature (°C)
T_m	mean temperature of air gap segment (°C), $T_m = (T_{ela} + T_{sla})/2$
T_s	temperature of preheated air blown into building (°C)
T_{sla}	outlet temperature of air gap (°C)
T_{se}	inside surface temperature of covering (°C)
T_{sext}	outside surface temperature of iron covering (°C)
T_{sint}	inside surface temperature of "Alubac" metal support (°C)
T_{sol}	mean soil temperature over a month (°C)
T_{spuits}	outlet temperature of buried pipe system (°C)
T_{surlv}	surface temperature of glass wool (°C)
ΔT	time step of calculation (h)
T_z	zone temperature (°C)

Greek symbols

ε	emissivity of glass wool and covering
σ	Stefan–Boltzmann constant (W/m^2 · K^4)
α	solar absorption coefficient
Φ	solar radiation on covering (W/m^2)
λ	conductivity coefficient (W/m · K)

*Laboratoire D'Etudes Thermique et Mecanique, INSA, Genie Civil, Complexe Scientifique de Rangueil, 31077 Toulouse, France.

1. INTRODUCTION

FOR the past 10 years, our laboratory has been working on real site modelling [1–7]. The aim of building a real site simulation is to carry out parameter sensitivity studies for thermal behaviour, energy consumptions and comfort conditions, by using predictive models on configurations which differ from the experimental ones.

For such a study we generally follow the different stages indicated below.

- It is first necessary to develop a simulation model as close as possible to physical reality.
- Then, we must compare results from calculations with experimental ones. This is called validation of the model and it must be performed with good accuracy on various parameters such as temperature and thermal balances. Moreover, on a real site we need to validate the model over a long period of experimental results because the climate changes all the time. In the present case, experimentation covered the two-year period of 1991 and 1992.
- It is finally possible to develop parameter sensitivity studies which can give more information about the advantages and weaknesses of the systems considered.

2. DESCRIPTION OF THE ENERGY SAVING SYSTEMS

The gymnasium was composed of three rooms: room 1, room 2, and annexes with changing rooms. Each of these rooms had a specific set point control temperature for heating in winter.

The gymnasium was equipped with two energy saving systems (Fig. 1).

The first one was a ventilated roof composed of, from the outside towards the inside of the building:

- metal covering (iron);
- forced ventilated air gap (0.08 m thick);
- insulation material (0.08 m thick) supported by metallic pieces called "Alubac".

The second system was an air–earth heat exchanger which was buried at a depth of 1.7 m beneath the ground surface of the gymnasium. The tubes of the heat exchanger were made of plastic and were of different diameters.

In winter, air coming from the ventilated roof was led through a non-insulated air pipe network to an air–earth heat exchanger before being blown into the building. In summer, air was directly extracted from the ventilated roof or from the buried pipe system to be expelled outside.

3. THEORETICAL STUDY

3.1. *Case of the ventilated air gap*

As the ventilated roof had a very low thermal mass, it was modelled in the steady state using a three-equation system. Each of these equations represents the thermal

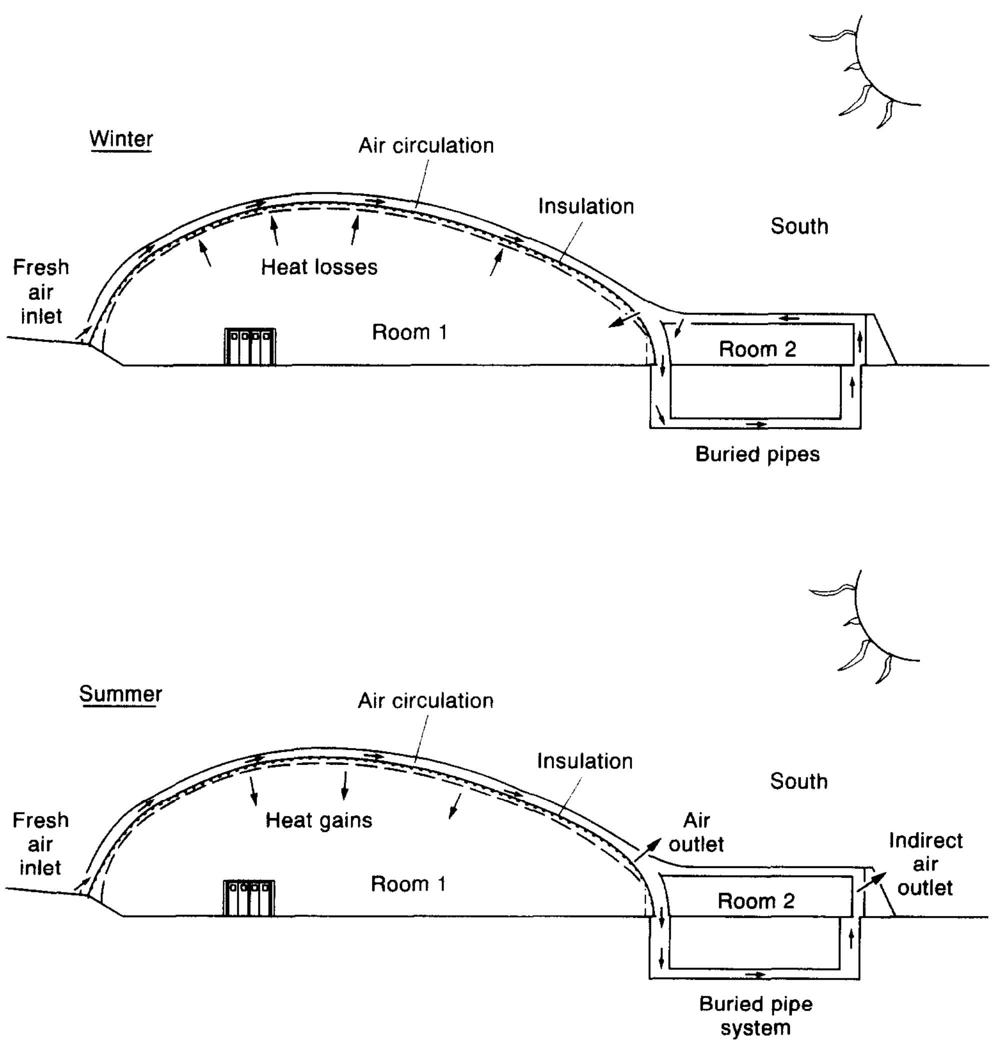

Fig. 1. Diagram of gymnasium's general ventilation.

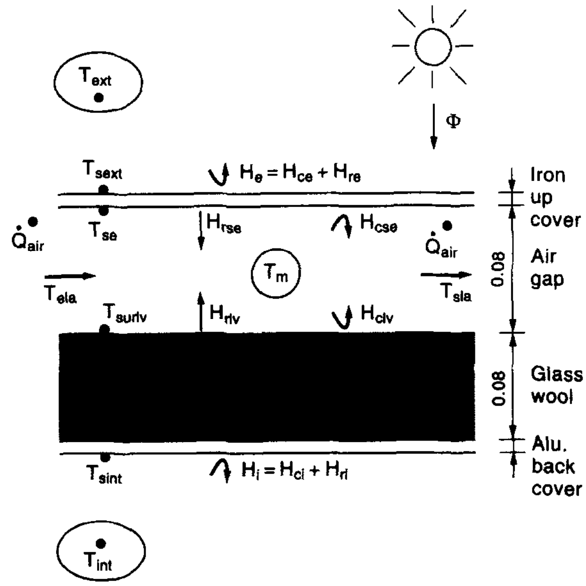

Fig. 2. Ventilated air gap thermal diagram.

balance of an air gap segment of the ventilated roof (Fig. 2).

$$-(H_{cse}+H_{rse}+1/R_e-1/R_e*1/(R_e*H_e+1))*T_{se} + H_{rse}*T_{surlv}+H_{ce}*T_m = -1/(1+R_e H_e)*(\alpha\Phi+H_e*T_{ext}) \quad (1)$$

$$H_{rlv}*T_{se}-(H_{rlv}+H_{clv}+1/R_i)*T_{surlv}+H_{clv}*T_m = -1/R_i*T_{sint} \quad (2)$$

$$H_{cse}*T_{se}+H_{clv}*T_{surlv}-(H_{cse}+H_{clv}+2m*C_p/L/L(i)*T_{ela}), \quad (3)$$

where $T_m = (T_{ela} + T_{sla})/2$.

This set of equations was solved by a Gauss–Seidel method using an iterative process to take into account the non-linearity of radiative heat exchange coefficients.

3.2. *Case of buried pipe system*

This type of installation is an old Persian concept which has existed for centuries. More recently, foreign and French authors have taken an interest in the performance levels of such systems [8–17]. They are used either to preheat fresh air in winter or to cool it in summer. However, generally speaking, air which goes into this pipe system comes directly from outside.

In our study this is not the case, because outside air flows first through the roof ventilated air gap, then into an air pipe network and finally into the buried pipe system itself (Fig. 3). Therefore, the performance of this buried pipe system can differ from that of the usual installations mentioned above. One of the goals of the present paper is to determine this performance.

To study the system, we developed a simplified model [17], taking the following into account:

- flow rates were small compared to the cross section of the buried pipes;
- the buried pipe system was not insulated and the ground temperature of the soil under the gymnasium followed the outside soil temperature at the same depth, but with a slight phase difference;
- the depth of the buried pipe system under the surface of the gymnasium was roughly 1.7 m, so we considered that the inside temperature of the gymnasium had no influence on the pipe system's thermal behaviour.

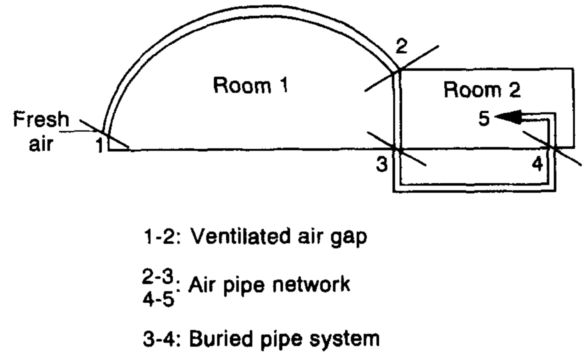

Fig. 3. Diagram of the different sections of the gymnasium ventilation system.

Consequently, we assumed that soil had a very high thermal mass and thus kept a constant temperature during the heat exchange. The thermal balance of a pipe segment can be represented as indicated in Fig. 4.

The final equation is the following:

$$T(x) = (T_o - T_{sol}) \times e^{(-x/m \times C_p \times R_{th})} + T_{sol}, \quad (4)$$

where R_{th} = overall thermal resistance, which can be expressed by the following relation:

$$R_{th} = \frac{1}{H_i \times P} + \frac{e}{\lambda \times P}$$

and T_{sol} = soil temperature around the tube, which we kept constant for each month (Table 1).

The tube internal convective exchange coefficient was determined using the relation defined in [18], under turbulent flow conditions.

$$\mathrm{Nu} = 0.023 \times \mathrm{Rey}^{0.8} \times \mathrm{Pr}^{0.4}. \quad (5)$$

We assumed that natural convection phenomena could be superposed on forced convection phenomena. Thus, the heat exchange coefficient of the ventilated air gap was calculated as follows [19]:

$$\mathrm{Nu} = 1.75[\mathrm{G_z}+0.012(\mathrm{G_z}\cdot \mathrm{G_r}^{1/3})^{4/3}]^{1/3}\cdot\left(\frac{\mu_b}{\mu_w}\right)^{0.14}, \quad (6)$$

where

μ_b = viscosity of air in middle of ventilated air gap
μ_w = viscosity of air near surfaces of air gap
$\mathrm{G_z}$ = Graetz number
$\mathrm{G_r}$ = Grashof number.

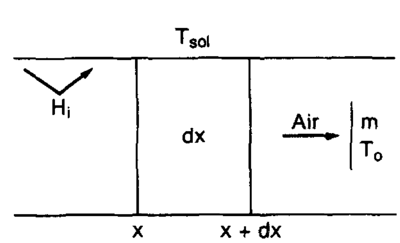

Fig. 4. Thermal balance of an elementary pipe segment.

Table 1. Soil average monthly temperature values (1.7 m depth) under ground surface of gymnasium from October 1991 to July 1992 for the real climatic site of Yzeure (France)

Month	October	November	December	January	February	March	April	May	June	July
Monthly temperature (°C)	17	15.1	12.6	11.6	12.4	14.3	15.4	17.3	19.6	20.3

4. VALIDATION OF MODELS

4.1. *Validation temperatures*

To validate the models we chose specific climatic sequences of 10 days length during 1992. The first one was a cold winter period of 1–10 February and the second one was a hot period of 1–10 June.

4.1.1. *Validation of ventilated roof model and air pipe network*. For architectural reasons, it was not possible to take the ventilated roof air outlet temperature directly. We measured it just before the entry to the buried pipe system. Consequently, this value of experimental temperature was influenced either by inside heat gains in winter or by thermal losses in summer, which occurred all along the non-insulated air pipe network going through the different rooms of the building.

Nevertheless, in our theoretical model, we took these air pipe heat exchanges into account, and we can see (Figs 5 and 6) that the experimental and theoretical temperature variations are in good agreement over the period studied. Discrepancy between these two values is generally lower than 1 K, except for a few hours during hot sunny days. For these cases, we think the errors come from our assumption that the roof thermal mass is negligible in our steady state model.

4.1.2. *Validation of buried pipe system model*. Once again, the discrepancy is small between the theoretical and experimental air outlet temperatures of the buried pipe system (Figs 7 and 8). Thus, the assumption of constant soil temperature during heat exchanges seems to be correct.

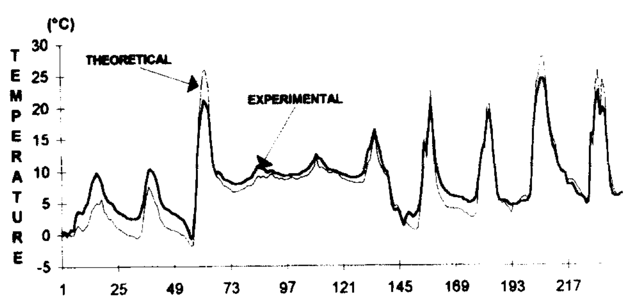

Fig. 5. Theoretical and experimental air temperature variations at the air pipe network outlet during the period 1–10 February 1992.

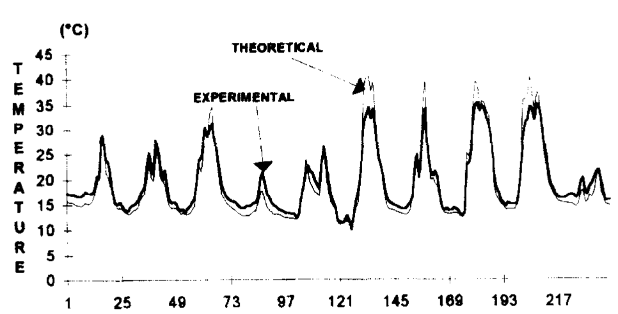

Fig. 6. Theoretical and experimental air temperature variations at the air pipe network outlet during the period 1–10 June 1992.

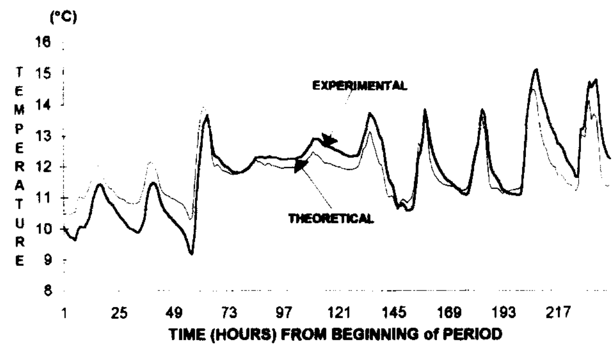

Fig. 7. Theoretical and experimental air temperature variations at the buried pipe system outlet during the period 1–10 February 1992.

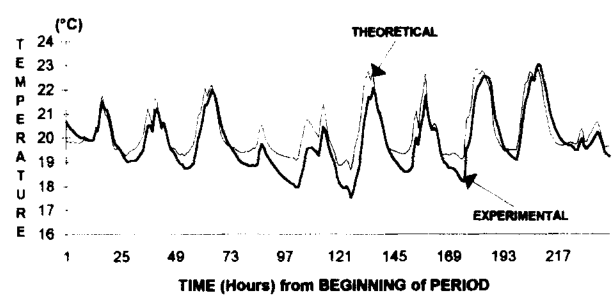

Fig. 8. Theoretical and experimental air temperature evolutions at the buried pipe system outlet during the period 1–10 June 1992.

4.2. *Thermal balance validations*

For the thermal balance validation of the models we chose a long measurement period, 1 November 1991 to 31 July 1992.

4.2.1. *Case of ventilated roof and air pipe network*. Results are presented for each month of the year (Table 2), and we can see that the difference between the theoretical and experimental results can vary significantly from one month to another. In fact, relative error for an individual month varies between 0 and 20%, but the total relative error value over the validation period is lower than 10%. We think that our model correctly represents the various heat exchanges which occur throughout the ventilated air gap and air pipe network.

However, as these results include two types of heat exchanges, we do not know exactly which energy comes from the ventilated air gap and which from the air pipe network. We give the balances in the paragraph corresponding to the sensitivity factor study.

Table 2. Thermal balance validation of ventilated roof and air pipe network for period 1991–1992

Month	Thermal balances (kWh) Experimental	Theoretical	Relative error (%), (exp − theor)/exp
November	2488	2013	19
December	3450	3161	8
January	3703	3424	8
February	3030	2777	8
March	3021	2476	18
April	3232	2747	15
May	3054	3050	0
June	1830	1691	8
July	1474	1624	−10
Total	25 282	22 963	9

4.2.2. *Case of buried pipe system.* We can see (Table 3) that the monthly theoretical results yielded by the model are as close to the experimental ones as they were for the ventilated roof. The relative error (column 4 of Table 3) varies within the same range, 0–20%. However, the global relative errors calculated both for positive values (energy collected from the soil) and for negative values (energy stored in the soil) are higher than in the case of the ventilated roof and air pipe network validation.

Many reasons can be evoked to explain this difference, particularly the fact that our simplified model does not take the inertia of the soil into account. However, we have to be aware that more sophisticated models which take the inertia of the soil into account can present a balance relative error of 10% [20].

Moreover, for our study it was not possible to measure soil properties other than the temperature value because this gymnasium was built 10 years before the experiments were carried out.

In spite of these difficulties, the assumption of a soil monthly temperature variation gives sufficient accuracy and the use of our simplified model is justified.

As a general conclusion of the validation, we can say that the two previous models were satisfactorily validated. However, before using them to develop a sensitivity factor study, we implemented them in the TRNSYS simulation environment [21]. A final verification was done, and we can check (Table 4) that the experimental and theoretical gymnasium global thermal balances over the heating period of 1991–1992 are very close, the relative error being lower than 4%.

Table 3. Thermal balance validation of buried pipe system for period 1991–1992

Month	Thermal balances (kWh) Experimental	Theoretical	Relative error (%), (exp − theor)/exp
November	1283	1064	17
December	1506	1320	12
January	1411	1167	17
February	841	714	15
March	510	409	20
April	260	264	2
May	−753	−638	15
June	−115	−98	15
July	−534	−447	16
Sum of positive values	5811	4938	15
Sum of negative values	−1402	−1183	16

Table 4. Global thermal validation of model in TRNSYS simulation environment over the heating period of the years 1991–1992

Gymnasium	Global thermal balance (kWh)
Experimental consumptions (kWh)	119 059
Theoretical consumptions (kWh)	124 066
Relative error, (exp − theor)/exp (%)	−4

5. RESULTS OF SIMULATION OBTAINED WITH NEW MODELS IMPLEMENTED IN TRNSYS SIMULATION ENVIRONMENT

5.1. *Energy values coming from roof and air pipe network of gymnasium*

We note that energy coming from the ventilated roof represents more than 70% of the global energy collected for the simulated year of 1992 (Table 5). However, energy gains coming from the air pipe network are not negligible, particularly in winter when the roof outlet air temperature is lower than the gymnasium heating temperature. Nevertheless, this energy is lost through the buried pipe system which is not insulated. On the contrary, in summer the energy recovered by the air pipe network is very low because the ventilated roof air outlet temperature is high. In this case, the air pipe network brings heat gains into the gymnasium and can affect the thermal comfort of the building.

To avoid these problems, we think that the air pipe network which goes through the different rooms of the gymnasium should be insulated.

5.2. *Values of energy collected by the roof*

The ventilated roof can collect energy in two ways:

- from heat lost by the gymnasium. This occurs mainly in winter, when the inside ambient temperature of

Table 5. Separated thermal balances of ventilated room and air pipe network of building for the year 1992

Period	Theoretical balance (kWh)	Ventilated roof (kWh)	Air pipe network (kWh)
November	2570	1065	948
December	3129	1821	1340
January	3334	2031	1393
February	3176	1822	955
March	3318	1618	858
April	2747	2099	648
May	3050	2726	324
June	1691	1418	273
July	1624	1530	94
Total	22 963	16 130	6833
	—	(70.2%)	(29.8%)

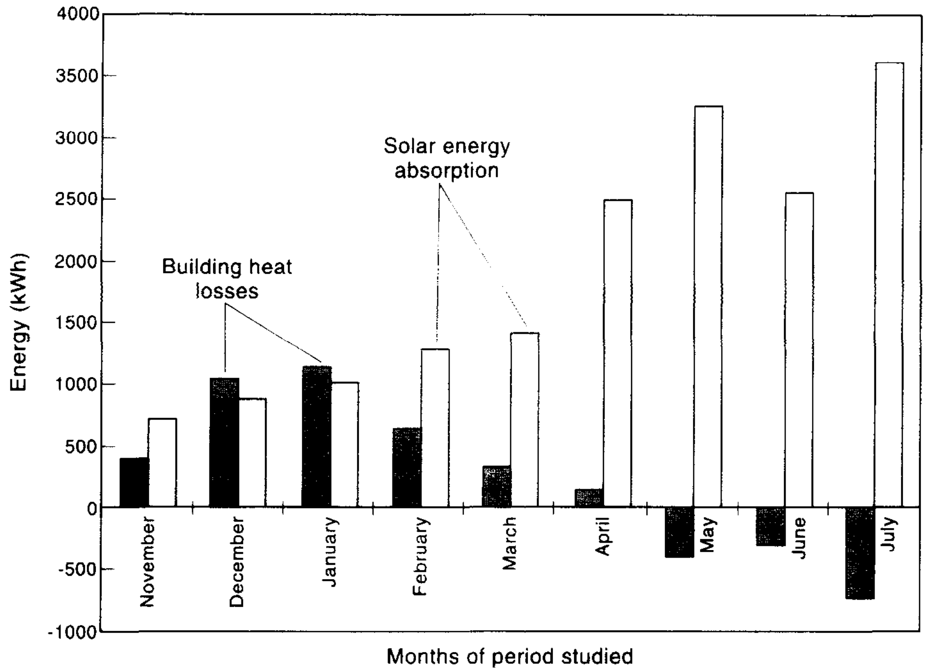

Fig. 9. Ventilated roof-collected energy coming from building heat losses and from top covering solar energy absorption during the period November 1991–July 1992.

Room 1 is greater than the air gap temperature. It is generally the case when outside climatic conditions are bad and when there is no sun;

- on sunny days when solar radiation on the iron covering is sufficient.

The authors thought that it would be interesting to know how much energy came from thermal losses and how much from solar energy absorption on the top cover. We can see (Fig. 9) that these two phenomena are not of equal importance.

Solar energy absorbed by the top covering during a whole year is greater than the energy collected from gymnasium thermal losses, except for two winter months. This result is quite understandable because the internal side of the roof is insulated and, of course, the top cover is not. Moreover, heating temperatures in the gymnasium are lower than in dwellings. So, thermal losses are lower too.

6. GLOBAL SENSITIVITY FACTOR ANALYSIS

6.1. *First sensitivity analysis*

6.1.1. *Presentation of results.* This study was carried out over a whole heating season, for the various cases indicated in the first column of Table 6:

- influence of the use of the buried pipe system for air renewal preheating: (1);
- influence of ventilation intermittency during the period when the gymnasium was not occupied: (2);
- influence of an increase of the ventilated roof insulation thickness (Th = 0.08 m): (3);
- combined influences of air pipe network insulation and regulation to blow air directly into the building when roof outlet temperature reaches a sufficient level. In this case, the air does not go through the buried pipe system: (4);
- influence of air pipe network insulation: (5);
- influence of regulation to blow air directly into building when roof outlet temperature reaches a sufficient level. In this case, the air does not go through the buried pipe system: (6);
- reference case for the whole sensitivity factor analysis: (7);
- influences of a solar absorption coefficient decrease for the ventilated roof covering: (8) and (9);
- combined influences of no air renewal preheating and of an insulation thickness increase (Th = 0.08 m) for the ventilated roof: (10);
- influence of no air renewal preheating: (11);
- combined influence of no air renewal preheating and of solar absorption coefficient decrease for the ventilated roof covering: (12);
- influence of the ventilated roof in air renewal preheating: (13).

6.1.2. *Simulation results.* Generally speaking, Table 6 shows that some parameters decrease gymnasium global consumptions [cases numbered (1) to (6)] and other parameters affect building energy performances, increasing consumptions [cases numbered (8) to (13)]. The most important difference which is recorded corresponds to the use of the buried pipe system for air renewal preheating [case (1)], and to the use of the ventilated roof for air renewal preheating [case (13)]. Compared to the reference case, (7), the first solution gives an energy gain and the second an energy loss.

It appears that the use of the buried pipe system to preheat fresh air is more efficient than the use of the ventilated roof.

We can also note that when there is no air renewal preheating (case 11), global gymnasium consumptions are lower than when this air is preheated by the use of

Table 6. Summary of preliminary sensitivity factor analysis

Simulation cases	Case number	Energy consumption (kWh) Room 1	Room 2	Annexes + changing rooms	Total	Relative value, (case − ref)/ref
Use of buried pipe system for preheating fresh air	(1)	26 305	3227	33 833	63 366	−16%
General ventilation intermittency influence	(2)	36 389	2727	25 578	64 694	−14%
Ventilated roof insulation increased influence (Th = 0.08 m)	(3)	33 972	3017	33 972	70 961	−6%
Combined influences of air pipe network insulation and regulation	(4)	35 833	2894	32 777	71 504	−5%
Air pipe network insulation influence	(5)	36 666	3158	33 972	73 796	−2%
Regulation influence	(6)	37 500	2748	32 750	72 998	−3%
Reference case	**(7)**	**38 222**	**3017**	**33 972**	**75 211**	**0%**
Solar absorption coefficient decrease (α = 0.6)	(8)	39 222	3075	34 056	76 353	2%
Solar absorption coefficient decrease (α = 0.0)	(9)	41 667	3231	34 306	79 204	5%
Combined influences of no fresh air preheating and ventilated roof insulation increase (Th = 0.08 m)	(10)	38 167	11 250	34 194	83 611	11%
Influence of no air renewal preheating	(11)	39 972	11 275	34 194	85 441	14%
Combined influences of no air renewal preheating and ventilated roof solar absorption coefficient decrease (α = 0.0)	(12)	43 583	11 358	34 389	89 331	19%
Roof ventilation influence for air renewal preheating	(13)	47 138	9688	33 278	90 104	20%

the ventilated roof (case 13). It should be remembered that the roof top cover is not transparent to solar energy radiation; it cannot be considered as a classical solar captor. Consequently, it presents a very poor global energy performance during the heating period.

Moreover, energy collected from building heat losses on cold days is not important, because the average ambient temperature of room 1 is within the range of 14–15°C and it does not take values as high as for a dwelling. Nevertheless, a more complete analysis is necessary to draw more accurate conclusions. We present this in the next section.

The influence of other parameters seems to be weaker, but not negligible, particularly the use of ventilation intermittency at night and also the improvement of room 1's roof insulation thickness, which lead to energy savings of 14% (case 2) and 6% (case 3) respectively.

6.2. *Influence of configuration used for the air renewal preheating*

6.2.1. *Conditions of simulation.* We simulated four different configurations for air renewal preheating (Fig. 10).

- The first one corresponds to the real configuration where air renewal preheating is accomplished by the coupled running of the ventilated roof and the buried pipe systems. We have called it "DYN" for dynamic configuration.
- The three other ones are simulation configurations, which differ by the way in which fresh air is preheated before being blown into the gymnasium. We have named them as follows:
  - "PITS" configuration when air is only preheated by the use of the buried pipe system;
  - "ROOF" configuration when air is only preheated by the use of the ventilated roof;
  - "STAT" for static configuration, because the roof of room 1 is not ventilated. For this case, there is no air renewal preheating and outside fresh air is directly introduced into the building.

It should be noted that for each of the study cases, the set point control temperature of rooms 1 and 2 varied within a range of 12–15°C, as provided for by French building regulations [22].

6.2.2. *Results of simulations.* The overall results of these simulations are presented in Table 7. We determined the following parameters for the different simulation configurations:

- column 1: the simulation number;
- column 2: the type of configuration for the different set point temperature values of rooms 1 and 2;
- column 3: the value of results given as follows:

$$Q = m\,C_p(T_s - T_z). \qquad (7)$$

Comments:

- T_z represents the value of the zone temperature calculated each hour by the simulation model;
- for the three configuration cases of ROOF, PITS and DYN, the parameter T_s is equal to the temperature of the air blown into the gymnasium after having crossed either the ventilated roof of room 1 or the buried pipe system, or both. The higher the value of T_s, the better the air is preheated. This parameter appears as an interesting means of studying the energy efficiency of these different configurations;
- for the STATIC configuration, the same parameter T_s was taken as equal to the outside air ambient temperature value and it can be used as a reference for the other three configurations;
- column 4: real heat losses by room 1's roof;
- columns 5, 6, 7: energy consumptions of room 1, of annexes and changing rooms and of room 2;
- column 8: gymnasium global consumptions for the cases studied with the simulation model;

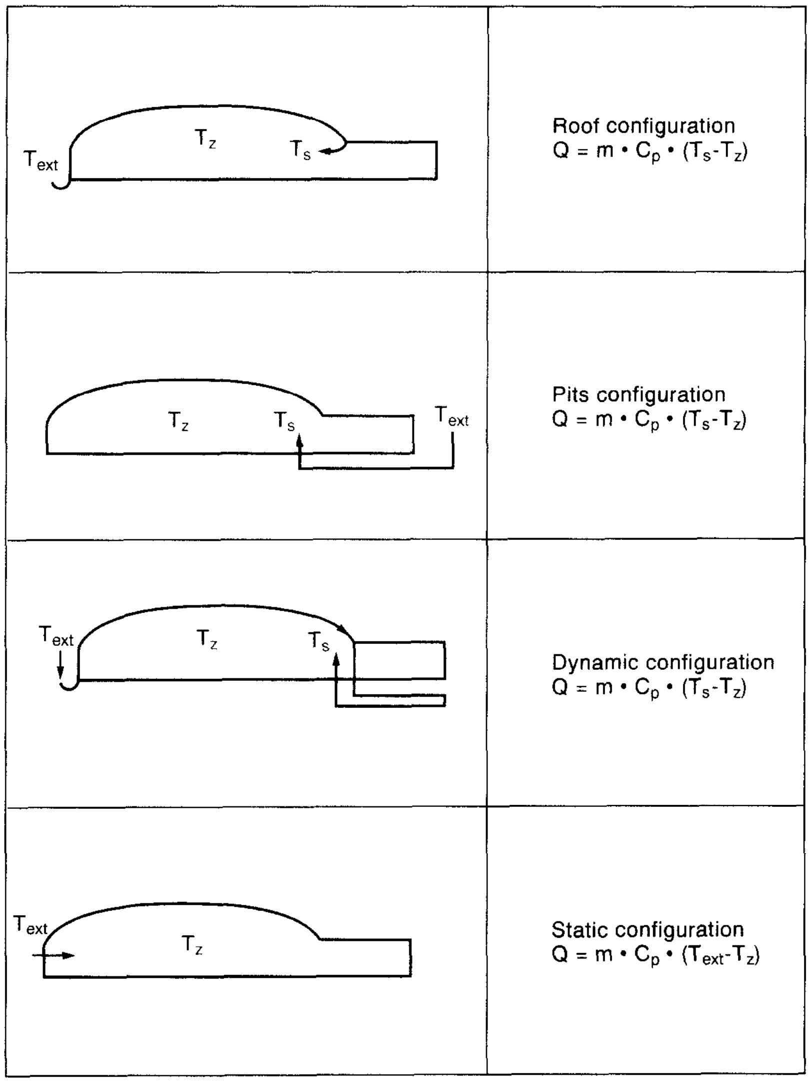

Fig. 10. Diagram of the different types of configurations simulated for the air renewal preheating.

Table 7. Summary table of the different heat losses and energy consumptions for the four types of configuration studied

Number	Type	Heat losses (kWh) Air renewal	Heat losses (kWh) Roof of room 1	Energy consumption (kWh) Room 1	Energy consumption (kWh) Annexes + changing rooms	Energy consumption (kWh) Room 2	Energy consumption (kWh) Building (total)	Relative difference, (case − ref)/ref (%)
1	STAT 12	31 269	4962	39 972	34 194	11 275	85 442	14%
2	STAT 13	34 540	6796	50 861	31 694	13 911	96 467	28%
3	STAT 14	37 977	8608	62 633	29 111	16 650	108 094	44%
4	STAT 15	41 542	10 543	74 222	26 450	19 461	120 133	60%
5	ROOF 12	18 319	22 878	47 139	33 278	9689	90 106	20%
6	ROOF 13	21 592	24 688	58 056	30 972	12 078	101 106	34%
7	ROOF 14	23 686	25 808	69 417	28 556	14 583	112 556	50%
8	ROOF 15	27 159	27 704	81 194	26 042	17 183	124 419	65%
9	PITS 12	3402	5174	23 306	33 833	3228	63 367	−16%
10	PITS 13	6217	6858	36 500	31 667	5403	73 569	−2%
11	PITS 14	9205	8655	47 417	29 194	7903	84 514	12%
12	PITS 15	12 307	10 548	58 889	26 550	10 586	96 025	28%
13*	**DYN 12**	**1055**	**22 001**	**38 222**	**33 972**	**3017**	**75 211**	**0%**
14	DYN 13	3982	23 763	49 361	31 806	5125	86 292	15%
15	DYN 14	6992	25 610	60 972	29 361	7564	97 897	30%
16	DYN 15	10 086	27 517	73 028	26 753	10 194	109 975	46%

*Reference case for calculation of relative difference.

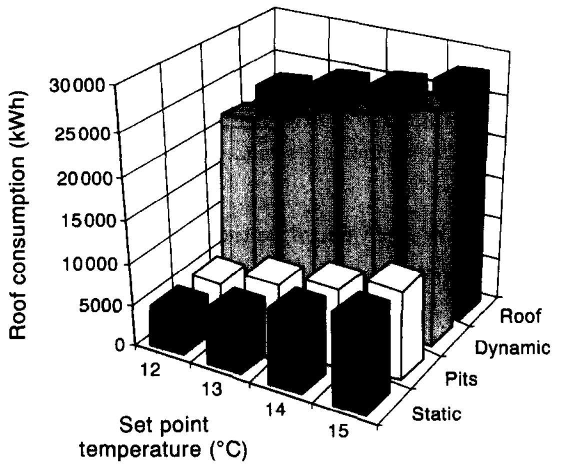

Fig. 11. Influence of set point temperature on roof thermal balance of room 1, for the four configuration types studied.

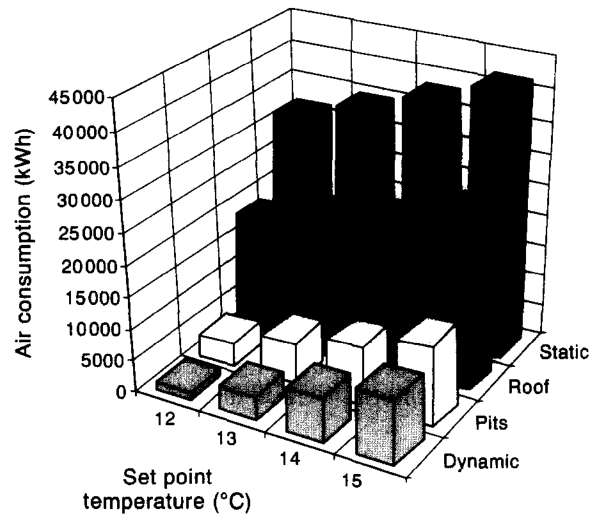

Fig. 12. Influence of set point temperature on global air renewal thermal balance of gymnasium for the four configuration types studied.

- column 9: relative variation, defined as follows:

$$\frac{\text{Global consumptions (simulation case} - \text{reference case)}}{\text{Global consumptions of the reference case}}. \quad (8)$$

As was foreseeable, we note that, for all configuration types in Table 7, the set point control temperature of rooms 1 and 2 has a significant influence on gymnasium global consumptions.

This table indicates the relative performance of the different configurations. In order of decreasing efficiency, they are as follows:

(1) PITS configuration;
(2) DYN (PITS + ROOF) configuration;
(3) STAT configuration;
(4) ROOF configuration.

These results confirm the analysis that we have just seen. The buried pipe system configuration is more interesting for preheating air than the ventilated air gap of room 1.

However, this does not give any information about these differences, so we outlined, for each configuration studied, the following:

- Fig. 11: values of roof heat losses of room 1;
- Fig. 12: values of air renewal heat losses of gymnasium;
- Fig. 13: values of global thermal balances defined by the sum of ventilated roof heat losses of room 1 and gymnasium air renewal consumptions.

We can see (Fig. 11) that roof heat losses are greatly increased for the two configurations where the air gap of room 1 is ventilated. For these two cases, the energy collected inside the air gap for preheating fresh air is too low, and cannot compensate the increase of roof heat losses of room 1 (Fig. 12).

For example, compare the thermal balances of the cases corresponding to "STAT 12" and "ROOF 12" (Table 8). We see that, although the use of the ventilated air gap can save roughly 13 000 kWh on air preheating, it leads to an increase in roof heat losses of 17 916 kWh. Thus, we obtain a total thermal loss of 4966 kWh.

So, the global thermal balance which is the algebraic

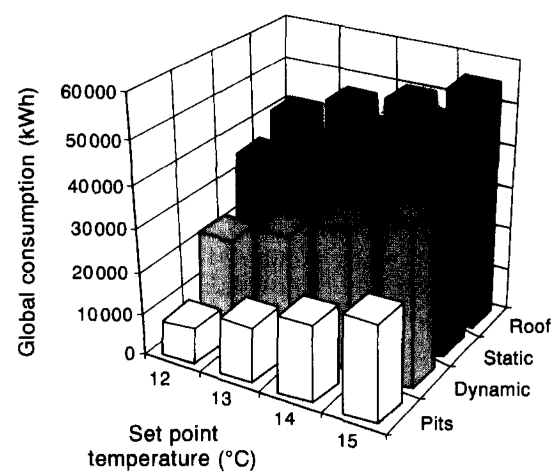

Fig. 13. Influence of set point temperature on global thermal balances (roof of room 1 + gymnasium air renewal) for the four configuration types studied.

sum of these two types of thermal balance, again shows the decreasing order of energy efficiency (Fig. 13).

Consequently, the ventilated air gap, as it is not a classical solar captor with greenhouse effect, presents a very poor thermal performance which cannot compensate for the increased thermal losses, particularly when ventilation is run during the night, as is the case for the installation considered.

Table 8. Compared thermal balances of ventilated roof heat losses and air renewal preheating for the static 12 and dynamic 12 configuration thermal balances (kWh)

Type of configuration	Thermal balances (kWh): Heat consumption for gymnasium air renewal (kWh)	Thermal balances (kWh): Consumption of room 1 (kWh)
STAT 12	31 269	4962
ROOF 12	18 319	22 878
Thermal balances	Gains = + 12 950	Losses = − 17 916
Global thermal balance	Final losses = − 4966 # − 5000	

Table 9. Air renewal flow rate values throughout the day

Air renewal	With ventilation (8 a.m.–10 p.m.)	Without ventilation (10 p.m.–8 a.m.)
Flow rate values (m^3/h)	2350	0

It should be noted that these conclusions are only true for permanent running of the ventilation and for the climatic site of Yzeure. What would happen if the ventilation was stopped during the night or if another climatic site was chosen? We shall discuss this in the next section.

7. OPTIMIZATION OF GYMNASIUM FRESH AIR INTRODUCTION

7.1. *The problem*

The aim is to blow fresh air into the gymnasium at the highest possible temperature.

First, we compared the different temperature values obtained when going (or not) through the different preheating systems for each time step of calculation. We kept the highest temperature value calculated by the model.

Second, we modulated the air renewal flow rate value (Table 9) according to:

- gymnasium occupation;
- comparison of air temperature values, T_s at the outlet of the preheating system considered and T_z the zone temperature.

Let us note that this study is not very realistic, unless the simulation program can be used as a predictive tool to pilot the gymnasium air ventilation system in real time.

7.2. *Conditions of simulation*

This study was carried out taking into account the following conditions:

- possibility of intermittent ventilation during the night;
- study performed for two climatic sites: Yzeure and Montpellier;
- study performed for two heating temperatures of rooms 1 and 2: 12 and 15°C;
- study carried out for only two types of configurations, the real configuration of the gymnasium (DYN) and the system which provided the highest energy economy (PITS).

7.2.1. *Case of the DYN configuration.* The DYN configuration is represented in Fig. 14.

- For the air preheating temperature value of T_s we took
  - T_s = maximum value of (T_{ext}, T_{stoit}, T_{spuits}).

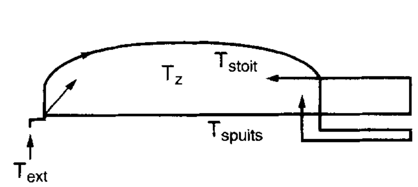

Fig. 14. Optimization diagram for DYN configuration.

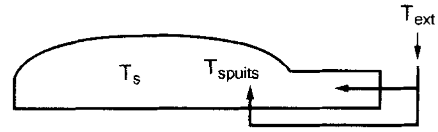

Fig. 15. Optimization diagram for PITS configuration.

- For the flow rate value m we took
  - during the day:
    - $m = 2350\,m^3/h$
  - during the night:
    - if $T_s > T_z$: $m = 2350\,m^3/h$
    - if $T_s < T_z$: $m = 0\,m^3/h$.

7.2.2. *Case of the PITS configuration.* The PITS configuration is represented in Fig. 15.

- For the air preheating temperature value of T_s we took
  - T_s = maximum value of (T_{ext}, T_{spuits}).
- For the flow rate value m we took
  - during the day: $m = 2350\,m^3/h$
  - during the night:
    - if $T_s > T_z$: $m = 2350\,m^3/h$
    - if $T_s < T_z$: $m = 0\,m^3/h$.

7.3. *Simulation results*

We can see from Figs 16 and 17 that the fresh air preheating optimization varies with the climatic site considered.

For the climatic site of Yzeure, if we compare the results obtained by optimization with those from the use

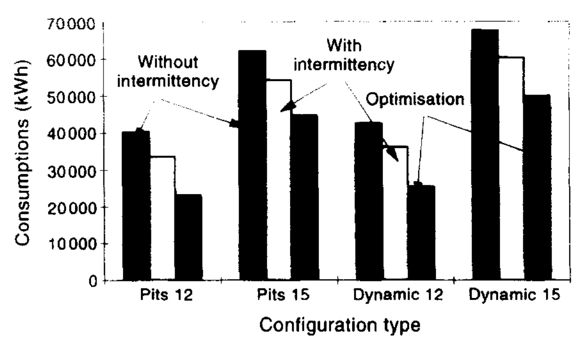

Fig. 16. Influence of fresh air preheating optimization on gymnasium global consumptions for the climatic site of Montpellier.

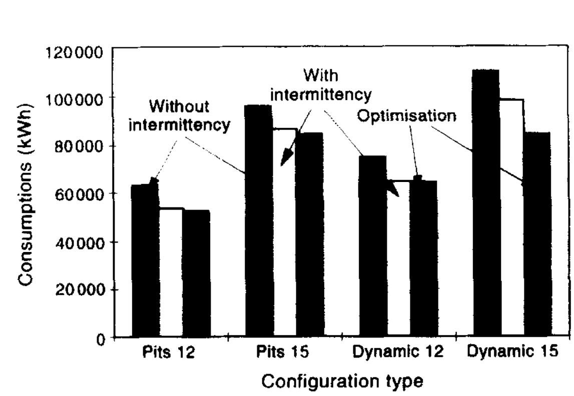

Fig. 17. Influence of optimization on gymnasium global consumptions for the climatic site of Yzeure.

Table 10. Comparative table of the principal characteristics of the climatic sites of Yzeure and Montpellier during the heating period 1991–1992

	Climatic site	
	Yzeure	Montpellier
Solar radiation	354 kWh/m^2	579 kWh/m^2
Degree hours relative to base 12	32 980	16 397

of ventilation intermittency alone, we can see that the optimization influence is very weak, except for the DYN 15 configuration (Fig. 16). Conversely, for the climatic site of Montpellier the optimization can save more energy than the use of ventilation intermittency alone (Fig. 17).

This difference comes directly from the difference in meteorological conditions between these two cities during the heating period (Table 10). The climate in Montpellier is warmer and sunnier than that in Yzeure, particularly if we compare the degree hours base 12. Thus, the temperature T_s more frequently exceeds the zone temperature value T_z, leading to a considerable decrease in energy consumption by the building.

8. CONCLUSION

This study points out the general interest of real site simulation with correctly validated models.

For this case, models can be used as a predictive tool to give more information about the advantages or disadvantages of components in system design and, finally, about dynamic performances of coupled energy saving systems.

With the help of a preliminary sensitivity factor analysis, we have first shown the best improvements which have to be made to save a large amount of energy. We conclude that the most significant parameters are the running parameters such as night ventilation intermittency, or component design parameters such as the use of a buried pipe system.

A systematic analysis of several air preheating configurations has pointed out the order of efficiency of the different air preheating systems. Thus, it appears that the use of an air–earth heat exchanger is a very appropriate solution for preheating fresh air in winter, even if its use is combined with another energy saving system such as a ventilated roof.

For the other solutions, particularly for the ventilated roof, we have to take into account the realities of the climatic site. For a rather cold climatic site, like that of Yzeure, gymnasium air introduction need not be optimized because this is not a means of saving energy. However, if the climate is warmer and sunnier, this solution can be used combined with ventilation intermittency.

Finally, we conclude that the use of simulation can be of great interest even for existing buildings which need energy saving improvements.

Acknowledgement—This study was supported by the French Agency for Environment Development and Energy Management (ADEME).

REFERENCES

1. Fabre, J., Etude en site réel d'une maison solaire passive à stockage de chaleur longue durée dans le sol. Thèse de Docteur Ingénieur de l'Université P. Sabatier, Toulouse, 1982.
2. Tepe, K., Contribution à l'étude du couplage thermique de locaux. Simulation et Experimentation. Thèse de Docteur Ingénieur de l'Université P. Sabatier, Toulouse, 1984.
3. Trombe, A., Pierson, P., Javelas, R. et groupe d'ingénieurs, *Guide A.I.C.V.F. Pratique de l'eau Chaude Sanitaire Solaire Individuelle*. Pyc Editions, Paris, 1985.
4. Baleynaud, J. M., Passive solar modelling. Validation and sensitivity study analysis. Thèse de Docteur Ingénieur de l'Université P. Sabatier, Toulouse, 1987.
5. Trombe, A., Javelas, R. and Petit, M., Etude expérimentale en site naturel du comportement thermique d'une dalle de sol sur terre plein. *Revue Générale de Thermique*, 1989, **328**, Avril.
6. Grenier, H., Javelas, R. and Trombe, A., Simulation en site réel du comportement thermique de matériaux semi-transparents. *Revue Genérale de Thermique*, 1989, **325**, Janvier.
7. Mavroulakis, A., Baleynaud, J. M. and Trombe, A., Dynamic processing of direct solar gains in TRNSYS simulation environment. *I.S.E.S. Solar World Congress*, Denver, CO, 19–23 August 1991.
8. Francis, C. E., Earth cooling tubes—case studies of three midwest installations. *Proceedings of Passive and Hybrid Cooling Conference*, Miami beach, FL, 1981, pp. 171–175.
9. Puri, V. M., Earth tube heat exchanger performance correlation using boundary element method. *Transaction of A.S.A.E.*, 1987, **30**(2), 514–521
10. Hendrick, P. L., Performance evaluation of a terrestrial heat exchanger. *Proceedings of the 5th National Passive Solar Conference*, Amherst, MA, 1980, pp. 732–736.
11. Abrams, D. W. and Benton, C. C., Simulated and measured performances of earth cooling tube. *Proceedings of the 5th National Passive Solar Conference*, Amherst, MA, 1980, pp. 737–741.
12. Spengler, R. W. and Stombaugh, D. P., An air–earth tunnel for cooling buildings. Optimization of earth tube heat exchangers for winter ventilation of swine housing. *Transactions of the A.S.A.E.*, 1983, **26**(4), 1187–1193.
13. Heinrich, E. and Isoardi, J. P., Rafraîchissement d'air par puits provençal. Document interne Costic, France, 1985.
14. Sodha, M. S., Sharma, A. K., Singh, S. P., Bansal, N. K. and Kumar, A., Evaluation of an earth–air tunnel system for cooling/heating hospital complex. *Building and Environment*, 1985, **20**(2), 115–122
15. Trombe, A., Bourret, B. and Petit, M., Expérimentation de Castanet. Rapport de contrat A.D.E.M.E. No. 1, Juillet 1991.

16. Trombe, A., Bourret, B., Soontorchainacksaeng, T. and Moreau, J. A., Expérimentation de L'I.N.S.A. Rapport de contrat A.D.E.M.E. No. 2, Juillet 1993.
17. Trombe, A., Benech, M. L., Romeu, G., Serres, L. and Mavroulakis, A., Expérimentation de l'Ariège. Rapport de contrat A.D.E.M.E final, Septembre 1993.
18. Bory, Ch., *Echanges de Chaleur par Convection*. Editions Bordas, Paris, 1980.
19. Necati Ozisik, M., *Heat Transfer: A Basic Approach*. McGraw-Hill, New York, 1990.
20. Soontornchainacksaeng, T., Etude expérimentale et théorique du comportement thermique d'un échangeur air–sol. Application à l'habitat individuel. Thèse de Docteur Ingénieur de L'I.N.S.A, Toulouse, 1993.
21. TRNSYS. Transient System Simulation Program. Manual Version 12.2. Solar Energy Laboratory, University of Wisconsin, Madison, WI, 1988.
22. Arrêté ministériel du 25 Juillet 1977. Limitation de la température de chauffage des locaux ou s'exercent des activités à caractère scientifique, sportif, artisanal, industriel, commercial et agricole, France, 1977.